

## Oxygenation Chemistry at a Mononuclear Copper(II) Hydroquinone System with O<sub>2</sub>

Kae Tabuchi, Hideki Sugimoto, Atsushi Kunishita, Nobutaka Fujieda, and Shinobu Itoh\*

Department of Material and Life Science, Division of Advanced Science and Biotechnology,  
Graduate School of Engineering, Osaka University, 2-1 Yamada-oka, Suita, Osaka 565-0871, Japan

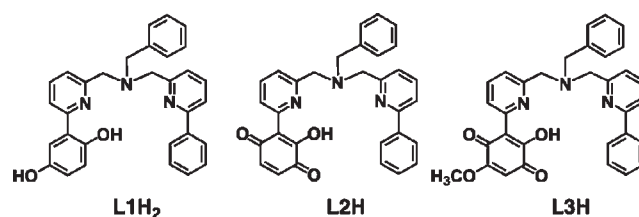
Received May 21, 2010

Aerobic treatment of a copper(II) complex supported by a bis(pyridin-2-ylmethyl)amine ligand containing a *p*-hydroquinone moiety on one of the pyridine donor groups in CH<sub>3</sub>OH induces oxygenation reaction of the ligand to give a hydroxylated *p*-quinone derivative.

In copper monooxygenases such as tyrosinase, peptidylglycine  $\alpha$ -hydroxylating monooxygenase, dopamine  $\beta$ -monooxygenase, and particulate methane monooxygenase, molecular oxygen (O<sub>2</sub>) is activated at a mono- or dinuclear copper reaction center to perform substrate oxygenation.<sup>1,2</sup> In the catalytic cycles of these enzymes, there is a distinct reduction process of copper(II) to copper(I) by an external reductant prior to O<sub>2</sub> binding and activation for the following substrate oxygenation.<sup>1–4</sup> The structure, physicochemical properties, and reactivity of several types of active oxygen species generated by the reaction of copper(I) complexes and O<sub>2</sub> have been studied extensively in model systems to provide significantly important insights into catalytic mechanisms of the copper monooxygenases.<sup>5,6</sup>

In copper dioxygenase such as quercetin 2,3-dioxygenase (2,3-QD), on the other hand, such a definite reduction process of the mononuclear copper(II) reaction center is not observed during the catalytic cycle. Thus, the enzymatic reaction is believed to involve *substrate activation* prior to O<sub>2</sub> binding. Namely, inner-sphere electron transfer from the deprotonated polyhydroxylated organic substrate (R<sup>–</sup>) to copper(II) initially occurs to generate an organic radical intermediate (R<sup>•</sup>) of the substrate and copper(I).<sup>7</sup> Then, the generated R<sup>•</sup>/copper(I) species readily reacts with O<sub>2</sub> having a triplet ground state (*S* = 1) to promote the substrate oxygenation reaction.<sup>7</sup> A similar

Chart 1



mechanistic scenario has been proposed for the biogenetic processes of a (trihydroxyphenyl)alanine quinone (TPQ) cofactor of copper-containing amine oxidase and a lysyltyrosylquinone (LTQ) cofactor of lysyl oxidase. In these cases, oxidative modification of the active-site tyrosine (precursor of the cofactor) is initiated by activation of tyrosinate (Tyr<sup>–</sup>, the deprotonated form of tyrosine) to a tyrosyl radical (Tyr<sup>•</sup>) via inner-sphere electron transfer to the active-site copper(II). Then, the generated Tyr<sup>•</sup>Cu<sup>I</sup> intermediate reacts with O<sub>2</sub> to induce the post-translational modification.<sup>8–11</sup> However, such substrate activation chemistry at a mononuclear copper(II) reaction center has been less investigated in model systems compared to the comprehensive copper(I) dioxygen model studies for the copper monooxygenase systems. In this Communication, we report a mononuclear copper(II) hydroquinone system, which undergoes a similar oxygenation reaction at its hydroquinone moiety to give hydroxylated *p*-quinone derivatives under aerobic conditions.

Ligand L1H<sub>2</sub> shown in Chart 1 (left) was synthesized according to the synthetic procedures described in the Supporting Information (SI; Scheme S1).<sup>12</sup> The copper(II) complex [Cu<sup>II</sup>(L1H)](ClO<sub>4</sub>) (Cu<sup>II</sup>L1H) was then prepared by treating the ligand and Cu<sup>II</sup>(ClO<sub>4</sub>)<sub>2</sub>·6H<sub>2</sub>O in acetonitrile. The crystal structure of Cu<sup>II</sup>L1H is shown in Figure 1, and the crystallographic data and selected bond lengths and angles are summarized in Tables S1 and S2 in the SI, respectively.

Compound Cu<sup>II</sup>L1H exists as a dimeric form in crystal, where one of the oxygen atoms of the hydroquinone moiety O1 bridges two copper(II) ions, making a Cu<sub>2</sub>O<sub>2</sub> rhombic

\*To whom correspondence should be addressed. E-mail: shinobu@mls.eng.osaka-u.ac.jp.

(1) Halcrow, M. A. *Monocopper Oxygenases*. In *Comprehensive Coordination Chemistry II*; Que, J. L., Tolman, W. B., Eds.; Elsevier: Amsterdam, The Netherlands, 2004; pp 395–436.

(2) Itoh, S. *Dicopper Enzymes*. In *Comprehensive Coordination Chemistry II*; Que, J. L., Tolman, W. B., Eds.; Elsevier: Amsterdam, The Netherlands, 2004; pp 369–393.

(3) Klinman, J. P. *Chem. Rev.* 1996, 96, 2541–2562.

(4) Solomon, E. I.; Sundaram, U. M.; Machonkin, T. E. *Chem. Rev.* 1996, 96, 2563–2606.

(5) Mirica, L. M.; Ottenwaelder, X.; Stack, T. D. P. *Chem. Rev.* 2004, 104, 1013–1045.

(6) Lewis, E. A.; Tolman, W. B. *Chem. Rev.* 2004, 104, 1047–1076.

(7) Pap, J. S.; Kaizer, J.; Speier, G. *Coord. Chem. Rev.* 2010, 254, 781–793.

(8) Klinman, J. P. *Proc. Natl. Acad. Sci. U.S.A.* 2001, 98, 14766–14768.

(9) Okeley, N. M.; van der Donk, W. A. *Chem. Biol.* 2000, 7, R159–R171.

(10) Dooley, D. M. *J. Biol. Inorg. Chem.* 1999, 4, 1–11.

(11) Brazeau, B. J.; Johnson, B. J.; Wilmot, C. M. *Arch. Biochem. Biophys.* 2004, 428, 22–31.

(12) Details of the experimental procedures are described in the SI.

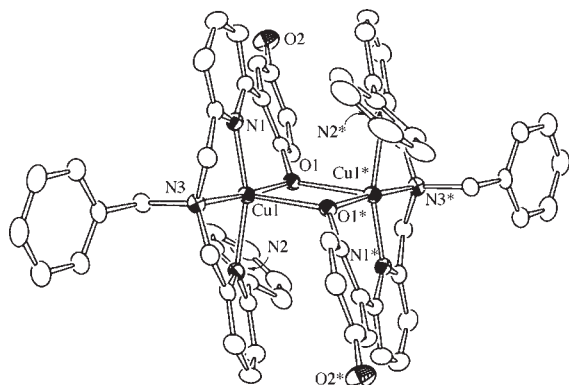


**Figure 1.** ORTEP drawing of  $\text{Cu}^{\text{II}}\text{L1H}$  showing 50% probability thermal ellipsoids. Counteranions, the solvent molecule, and hydrogen atoms are omitted for clarity.

core [ $\angle \text{O1}-\text{Cu1}-\text{O1}^* = 81.43(8)^\circ$  and  $\angle \text{Cu1}-\text{O1}-\text{Cu1}^* = 98.58(7)^\circ$ ]. The copper ion exhibits a distorted square-pyramidal geometry ( $\tau = 0.22$ ),<sup>13</sup> where the three nitrogen atoms N1, N2, and N3 and the oxygen atom O1 from the same ligand occupy the corners of the basal plane and the oxygen atom O1\* from another copper(II) monomer unit possesses the axial position [the  $\text{Cu1}-\text{O1}^*$  distance is 2.463(2) Å]. Because there is only one counteranion  $\text{ClO}_4^-$  per monomer unit, the hydroquinone oxygen atom O1 directly coordinating to the copper ion is deprotonated [ $\text{Cu1}-\text{O1}$  distance is 1.893(2) Å], whereas another oxygen atom, O2, is protonated, thus making the ligand monoanionic.

The electron spin resonance (ESR) spectrum of  $\text{Cu}^{\text{II}}\text{L1H}$  was taken in  $\text{CH}_3\text{OH}$  at 77 K, as shown in Figures S3 in the Supporting Information, which exhibited a typical spectrum of copper(II) with a tetragonal geometry ( $g_\perp = 2.074$ ,  $g_\parallel = 2.245$ , and  $A_\parallel = 155$  G). However, the peak intensity was relatively weak, and double integration of the ESR spectrum indicated that the spin density of the solution was  $\sim 40\%$ . These results indicated that there was an equilibrium between the monomeric and dimeric forms in solution, where the dimeric complex might be ESR-silent because of antiferromagnetic interaction between the two copper(II) ions bridged by the phenolic oxygen atoms (Figure 1).

To examine the  $\text{O}_2$  reactivity of  $\text{Cu}^{\text{II}}\text{L1H}$ , the complex was treated in methanol under a  $\text{O}_2$  atmosphere. Figure 2 shows a UV-vis spectral change of the reaction at room temperature. The relatively intense ligand-to-metal charge-transfer band at 410 nm ( $\epsilon = 1830 \text{ M}^{-1} \text{ cm}^{-1}$ ) due to  $\text{Cu}^{\text{II}}\text{L1H}$  gradually shifted to 458 nm ( $\epsilon = 540 \text{ M}^{-1} \text{ cm}^{-1}$ ) without any isosbestic point between the two absorption bands (410 and 458 nm). Thus, the reaction may involve several steps. Such a spectral change was not observed at all in the absence of  $\text{O}_2$ , clearly demonstrating that  $\text{O}_2$  was involved to initiate the reaction.

Then, we tried to isolate products from a preparative-scale reaction in methanol (see the SI). When the reaction was quenched after 15 min, the initial product  $[\text{Cu}^{\text{II}}(\text{L2})](\text{ClO}_4)$  ( $\text{Cu}^{\text{II}}\text{L2}$ ) having a molecular weight of 549.1345 was obtained in 77% yield. The molecular weight of this product is larger than that of the starting material  $\text{Cu}^{\text{II}}\text{L1H}$ , 535.1337, by 14 mass units, suggesting that both monooxygenation (one oxygen-atom insertion) and dehydrogenation ( $\text{H}_2$  elimination) reactions took place. Then, the organic product (modified

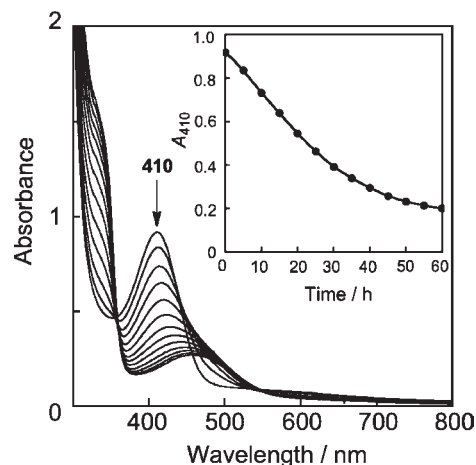


**Figure 2.** Spectral change observed upon introduction of an  $\text{O}_2$  gas into a methanol solution of  $\text{Cu}^{\text{II}}\text{L1H}$  (0.5 mM) at room temperature. Inset: Time course of the absorbance change at 410 nm.

ligand  $\text{L2H}$ ) was isolated by an ordinary workup treatment (demetalation) using an  $\text{NH}_3$  aqueous solution and following  $\text{SiO}_2$  column chromatography. Figure S4 in the SI shows the  $^1\text{H}$  NMR spectrum of modified ligand  $\text{L2H}$ , where there are two doublet peaks at  $\delta$  6.65 and 6.71, which are magnetically coupled to each other with  $J = 10.0$  Hz. Thus, there are two neighboring olefinic protons in  $\text{L2H}$ . In addition, there is a broad peak at  $\delta$  6.32, which disappeared upon the addition of  $\text{D}_2\text{O}$ . In the  $^{13}\text{C}$  NMR shown in Figure S5 in the SI, two distinct carbonyl carbon atoms are observed at  $\delta$  183.8 and 184.2. Furthermore, in the IR spectrum, there are two  $\text{C}=\text{O}$  stretching vibration peaks at 1682 and 1632  $\text{cm}^{-1}$ , together with an intense  $\text{O}-\text{H}$  vibrational peak at 3417  $\text{cm}^{-1}$ . On the basis of these spectral data, together with the detailed 2D NMR analyses (HSQC,  $\text{HH}-\text{COSY}$ , and  $\text{HMBC}$ ) shown in Figure S6 in the SI, the structure of the modified ligand  $\text{L2H}$  has been confirmed, as shown in Chart 1 (middle), and all of the  $^1\text{H}$  and  $^{13}\text{C}$  NMR peaks have been completely assigned, as indicated in Figures S4 and S5 in the SI, respectively.

When the aerobic reaction of  $\text{Cu}^{\text{II}}\text{L1H}$  was carried out for a prolonged time (3 days), the methanol adduct  $[\text{Cu}^{\text{II}}(\text{L3})](\text{ClO}_4)$  ( $\text{Cu}^{\text{II}}\text{L3}$ ) having a molecular weight of 579.1234 was obtained as a major product (61% yield; see the Experimental Section). An isotope labeling experiment using  $^{18}\text{O}_2$  unambiguously demonstrated that one of the oxygen atoms in the complex originated from  $\text{O}_2$  (Figure S7 in the SI).<sup>14</sup> In this case as well, the structure of the modified ligand  $\text{L3H}$ , which was isolated by demetalation and  $\text{SiO}_2$  column chromatography, has been determined as indicated in Chart 1 (right) by the IR,  $^1\text{H}$  NMR (Figure S8 in the SI),  $^{13}\text{C}$  NMR (Figure S9 in the SI), and 2D NMR ( $\text{HSQC}$ ,  $\text{HH}-\text{COSY}$ , and  $\text{HMBC}$ ; Figure S10 in the SI) analyses.

Furthermore, from an acetone/ $\text{CH}_3\text{CN}$  (5:1, v/v) solution of  $\text{Cu}^{\text{II}}\text{L3}$ , another copper(II) complex,  $[\text{Cu}^{\text{II}}(\text{L4H})](\text{ClO}_4)$  ( $\text{Cu}^{\text{II}}\text{L4H}$ ), crystallized after several days. The crystal structure of  $\text{Cu}^{\text{II}}\text{L4H}$  is presented in Figure 3, and the crystallographic data and selected bond lengths and angles are listed in Tables S1 and S2 in the SI, respectively. As is clearly seen in

(14) Computer simulation of electrospray ionization mass spectrometry obtained with  $^{18}\text{O}_2$  indicated that only 44%  $^{18}\text{O}$  was incorporated into the product. Such a relatively low value of  $^{18}\text{O}$  incorporation may be due to an exchange reaction of the OH group with  $\text{H}_2\text{O}$  in the solvent through a similar mechanism, as shown in Scheme 2.

(13) Addison, A. W.; Rao, T. N.; Reedijk, J.; van Rijn, J.; Verschoor, G. C. *J. Chem. Soc., Dalton Trans.* **1984**, 1349–1356.

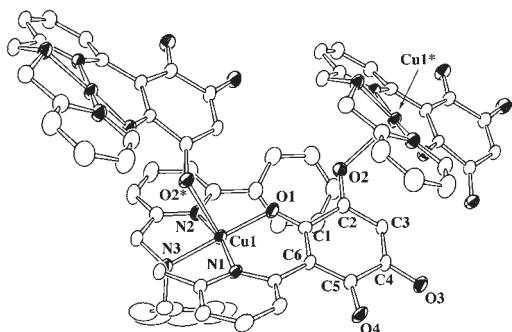
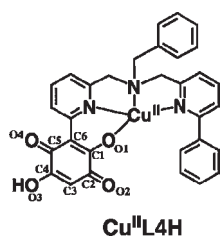


**Figure 3.** ORTEP drawing of  $\text{Cu}^{\text{II}}\text{L4H}$  showing 50% probability thermal ellipsoids. Counteranions and hydrogen atoms are omitted for clarity.

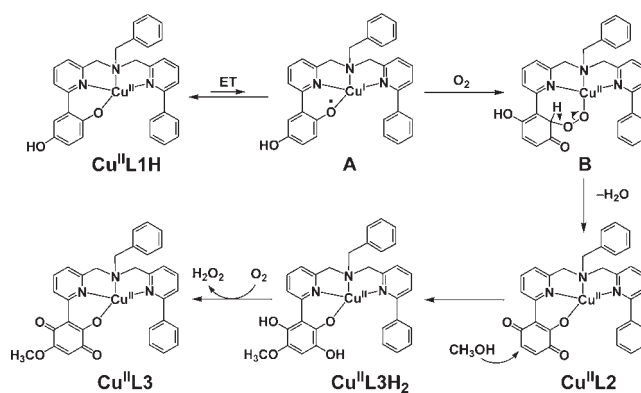
**Chart 2**



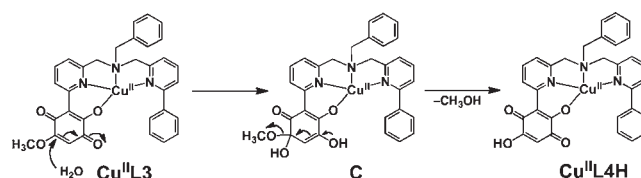
the crystal structure, the  $-\text{OCH}_3$  group in compound  $\text{Cu}^{\text{II}}\text{L3}$  is replaced by the  $-\text{OH}$  group in  $\text{Cu}^{\text{II}}\text{L4H}$  and one of the oxygen atoms, O1, of the modified ring consists of the equatorial plane, together with the three nitrogen atoms N1, N2, and N3 of the supporting ligand. Another oxygen atom of the modified ring, O2, acts as an axial ligand for another copper(II) complex,  $\text{Cu1}^*$  [ $\text{O2}-\text{Cu1}^* = 2.439(2) \text{ \AA}$ ], completing the square-pyramidal geometry of each copper(II) center ( $\tau = 0.10$ ).<sup>13</sup> Thus, in the crystal, oxygen atom O2 on the modified ring bridges the neighboring copper(II) complexes, constructing a one-dimensional polymer chain structure (see Figure S2 in the SI). Because there is only one counteranion  $\text{ClO}_4^-$  per monomer unit of complex  $\text{Cu}^{\text{II}}\text{L4H}$ , the modified ligand exists as a monoanionic compound (only one OH group is deprotonated). Judging from each C–O and C–C bond length (in  $\text{\AA}$ ) of the quinone moiety [C1–O1, 1.266(5); C2–O2, 1.228(5); C4–O3, 1.328(5); C5–O4, 1.229(5); C1–C2, 1.531(5); C2–C3, 1.449(5); C3–C4, 1.330(6); C4–C5, 1.507(5); C5–C6, 1.445(5); C6–C1, 1.392(5)], the most plausible canonical form of the modified ring in  $\text{Cu}^{\text{II}}\text{L4H}$  is the one depicted in Chart 2.

A possible mechanism for the formation of complexes  $\text{Cu}^{\text{II}}\text{L2}$  and  $\text{Cu}^{\text{II}}\text{L3}$  from  $\text{Cu}^{\text{II}}\text{L1H}$  is shown in Scheme 1, where a monomeric form dissociated from the dimer in the solution is considered as the reactive starting material because of its coordinatively unsaturated structure. Inner-sphere electron transfer from the deprotonated hydroquinone moiety to copper(II) in  $\text{Cu}^{\text{II}}\text{L1H}$  may generate a transient copper(I) semiquinone radical intermediate, **A**. Then,  $\text{O}_2$  attacks **A** to generate an alkylperoxo-type intermediate, **B**, from which heterolytic cleavage of the O–O bond may occur to give the quinone derivative  $\text{Cu}^{\text{II}}\text{L2}$ .

**Scheme 1.** Possible Mechanism for the Formation of  $\text{Cu}^{\text{II}}\text{L2}$  and  $\text{Cu}^{\text{II}}\text{L3}$



**Scheme 2.** Possible Mechanism for the Formation of  $\text{Cu}^{\text{II}}\text{L4H}$



In the prolonged reaction time, Michael addition of the solvent molecule methanol occurs at one of the nonsubstituted olefinic carbon atoms to give  $\text{Cu}^{\text{II}}\text{L3H}_2$ , which is further oxidized by  $\text{O}_2$  to give  $\text{Cu}^{\text{II}}\text{L3}$ . During the recrystallization process, hydrolysis of  $\text{Cu}^{\text{II}}\text{L3}$  may take place through intermediate **C** to give  $\text{Cu}^{\text{II}}\text{L4H}$  (Scheme 2).

In summary, the  $\text{O}_2$  reactivity of a copper(II) hydroquinone system,  $\text{Cu}^{\text{II}}\text{L1H}$ , has been examined to demonstrate that the substrate activation could occur to induce oxidative modification of a hydroxylated aromatic group at a mononuclear copper reaction center. The reaction may involve the key steps of TPQ and LTQ biogenesis such as inner-sphere electron transfer, generating an organic radical copper(I) species, formation of an alkylperoxocopper(II) intermediate, and Michael addition of the solvent molecules. Further mechanistic studies are now in progress using a series of phenol-containing ligands.

**Acknowledgment.** This work was financially supported by Grants-in-Aid for Science Research on Priority Areas (Grant 200360044, Synergy of Elements; Grant 21108515,  $\pi$ -Space) from Ministry of Education, Culture, Sports, Science and Technology, Japan, and also by the Asahi Glass Foundation and Mitsubishi Foundation. We also thank Dr. Kyoko Inoue of the analytical center of Osaka University for her assistance in obtaining the 2D NMR data.

**Supporting Information Available:** Further details are given in Tables S1 and S2, Figures S1–S10, and in a CIF file. This material is available free of charge via the Internet at <http://pubs.acs.org>.